

Title No. 115-M51

Effects of Moisture, Temperature, and Freezing and Thawing on Alkali-Silica Reaction

by Richard A. Deschenes Jr., Eric R. Giannini, Thanos Drimalas, Benoit Fournier, and W. Micah Hale

Alkali-silica reaction (ASR) and freezing and thawing (F/T) deterioration reduce the service life of concrete. The influence of relative humidity (RH), temperature, wetting-and-drying (W/D), and F/T on the development of ASR were evaluated herein. These factors exacerbate concrete deterioration, and understanding the relationship between moisture and deterioration is necessary for mitigation. The results of this study confirm a relationship between deleterious expansion and environmental conditions such as moisture and temperature. The results confirm the aggravating effect of F/T on ASR. The results indicate that sufficient drying may prevent both ASR and F/T deterioration in non-air-entrained concrete. Silane was evaluated as a mitigation measure for concrete exposed to a combination of ASR, F/T, and W/D and found to increase drying.

Keywords: alkali-silica reaction (ASR); freezing and thawing (F/T); mitigation; relative humidity (RH); silane; wetting and drying.

INTRODUCTION

Alkali-silica reaction (ASR) and freezing-and-thawing (F/T) deterioration in concrete are both related to the moisture state of concrete. ASR deterioration occurs when moisture within the pore solution is absorbed into alkali-silica gel, resulting in expansive pressure and cracking. The F/T deterioration mechanism occurs when water within the cement paste or aggregate pores freezes repeatedly and exerts pressure on the cement paste, causing cracking. The ambient conditions to which concrete is subjected affect the moisture state within the concrete, which influences the development of expansive pressures and deterioration.

Alkali-silica reaction (ASR)

ASR occurs when alkali cations (Na^+ and K^+) within the pore solution free hydroxyl ions (OH^-), which interact with silanol groups of siliceous phases found in certain aggregates.¹ Siliceous phases are transitioned into water-insoluble gel products composed of calcium, alkalis, and dissolved silica.¹ Cations (K^+ , Na^+ , Ca^{++}) further penetrate the silica structure, hydrolyzing siloxane bonds and allowing the reaction to proceed.² The rate of reaction depends on the concentration of cations in the pore solution. The reaction rate also depends on the solubility of silica, which is a function of the silica structure and texture, and the temperature. Siliceous phases may range from ordered quartz to amorphous silica, with ordered minerals being less soluble and requiring higher alkalinity and temperature to dissolve. Chalcedony, opal, and amorphous silica (for example, volcanic glass) are increasingly disordered and dissolve faster.

Expansion occurs by osmosis due to the solute concentration gradient between the water-insoluble alkali-silica gel

and the cement paste pore solution.³ Expansion may lead to microcracks in the aggregate particles and cement paste, which extend to form a network of microcracks. Bérubé et al.⁴ and Nishibayashi et al.⁵ observed that cycles of wetting-and-drying (W/D) may cause surface cracking. The cycles impart a moisture and alkali gradient between the bulk concrete and the exposed surface, and the surface expands less relative to the bulk concrete, causing macrocracking at the surface.^{4,6,7}

Freezing and thawing (F/T)

F/T deterioration occurs when pressure develops within the capillary spaces of the cement paste during cooling. The exact mechanism by which F/T stress occurs is complicated by the colloidal nature of the cement paste and the concentration of cations within the pore solution. Powers⁸ postulated that pressure develops when pore water is transported through the cement due to freezing. Powers and Helmuth⁹ later found that water moves by osmosis toward the formation of ice due to a free-energy gradient. Deterioration occurs when pressure develops in the capillary spaces due to viscous resistance to water transport.^{10,11} A threshold distance exists over which water can be transported before deterioration occurs.¹⁰ Air entrainment can be used to protect concrete from F/T distress and provides a network of small, dispersed voids with a spacing factor of approximately 0.006 in. (2.4×10^{-4} mm).¹⁰ In non-air-entrained concrete, the symptoms of distress materialize as cracks and spalling, which track parallel to the exposed surface of the concrete.

F/T-related deterioration can also arise due to water diffusion from aggregate particles.¹⁰ Litvan¹² postulated that pressure develops as relative humidity (RH) decreases in the aggregate pores, and water diffuses into the cement paste, thereby inducing stresses on the capillary spaces in the cement.¹¹ Typically, aggregate particles contain pores and capillary networks larger than those of the cement paste and are not saturated after hydration of the cement.¹⁰ F/T-susceptible aggregates have fine, interconnected pores and higher permeability than the adjacent cement paste. Therefore, water cannot disperse into the less-permeable cement paste on rapid freezing. When the aggregate particles become fully saturated before freezing, water may be expelled into

ACI Materials Journal, V. 115, No. 4, July 2018.

MS No. M-2017-273.R1, doi: 10.14359/5170219, was received August 9, 2017, and reviewed under Institute publication policies. Copyright © 2018, American Concrete Institute. All rights reserved, including the making of copies unless permission is obtained from the copyright proprietors. Pertinent discussion including author's closure, if any, will be published ten months from this journal's date if the discussion is received within four months of the paper's print publication.



Fig. 1—Concrete pavement D-cracking, Interstate 49.

the surrounding cement paste by hydraulic pressure.¹⁰ On repeated F/T, microcracking may develop within the interfacial transition zone (ITZ) and extend until a network of macrocracks form. In jointed concrete pavements, cracks may form at the pavement edges and curve along the corners, forming a D-shape, known as D-cracking (Fig. 1). To prevent F/T deterioration in concrete, susceptible aggregates must not remain saturated after initial drying or become saturated on exposure to external moisture.¹⁰

ASR and F/T

As noted by Bérubé et al.⁴ a combination of ASR and F/T deterioration can occur in concrete. Concrete cylinders exposed to ASR and W/D had a 2-year expansion of 0.13% as compared to 0.20% for cylinders exposed to a humid environment.⁴ However, cylinders exposed to W/D experienced greater map cracking. Air-entrained concrete cylinders exposed to ASR-accelerating conditions followed by cyclic F/T expanded more (0.26%) than cylinders exposed to ASR-accelerating conditions alone (0.20%). The cylinders continued to expand due to microcracking even after ASR deterioration slowed. The 2-year expansion in non-air-entrained concrete cylinders exposed to the same ASR and F/T conditions was 0.34%. In comparison, cylinders without existing ASR deterioration exhibited no F/T deterioration and less than 0.04% expansion after 2 years. The hypothesized mechanism of combined ASR and F/T deterioration occurs when cracking initiated by ASR provides an avenue for water to penetrate the concrete, which may lead to saturation of the cement paste and aggregates.⁴ A network of cracks forms along the exposed surface and the permeability of concrete increases, decreasing the resistance to ASR and F/T deterioration. The concrete is maintained at a higher moisture state closer to saturation, further reducing resistance to F/T.⁴

Moisture state of concrete

Relationships between moisture and internal RH are typically used to quantify the moisture state of concrete in the field. RH is determined from the ratio of vapor pressure (VP) to the saturation VP of the same air-water solution (at

the same temperature). The saturation VP is calculated as a function of temperature, and VP is measured using a resistive or capacitive hygrometer (RH probe). RH probes can be embedded within a concrete element and output the internal RH and temperature of the concrete element.^{4,13-16} Modern digital RH recording devices can report RH, temperature, and VP. Due to the temperature dependence of RH, the corresponding internal temperature should be reported, and the RH should only be compared to RH values measured at similar temperatures.¹⁶

The nature of VP (and RH) within concrete is complicated by the colloidal nature of cement paste. The sorption characteristics of concrete are dependent on the tortuosity and size of capillary and interlayer pore spaces. Concrete absorbs water as ambient VP increases and desorbs water as ambient VP decreases. On drying, water evaporates first from larger cement pores where less energy is required for evaporation, and then from smaller cement pores. As this occurs, the internal VP decreases due to the pronounced curvature of water-menisci in the smaller cement pores.^{15,17,18} This process continues until the concrete is in equilibrium with the ambient conditions. When temperature increases, and the absolute volume of moisture within the concrete is held constant, internal VP increases due to the excitation of water and reduced surface tension.¹⁵ Additionally, water in the colloidal cement paste is transported from the capillary and interlayer spaces into the cement pores, thereby reducing the curvature of the water-menisci and increasing VP.¹⁷ This increase in internal VP with temperature is opposite to the process for noncolloidal materials.¹⁷ The relationship between internal VP and moisture content in concrete is therefore dependent on material properties such as hydration age and pore distribution. Although sorption isotherms can be developed by measuring mass change and internal VP as concrete dries, it is impractical to develop such relationships for each concrete structure.

Measuring RH in concrete

To better understand the relationship between internal RH and moisture state in concrete, Gause¹⁷ evaluated the drying characteristics of a 0.64 water-cement ratio (*w/c*) concrete. Internal RH and moisture content were monitored for 300 days within concrete samples (12 in. [305 mm] cubes). A hygrometer was embedded within the concrete and allowed to equilibrate with the concrete over time. The samples were sealed on five sides, and drying occurred only through the exposed face. Depending on the initial moisture condition of the samples, the internal RH at 1.5 and 3 in. (38 and 76 mm) were within 10% of the ambient conditions within 300 days, whereas the RH at 6 in. (152 mm) was up to 40% higher than ambient. The results demonstrate the effects of permeability and surface area on the rate of drying and equilibrium in concrete. Several years of drying may be required before internal RH reaches equilibrium with ambient RH for larger specimens. However, equilibrium may occur rapidly (less than 300 days) for elements smaller than 6 in. (152 mm) and exposed to drying from multiple sides.

Stark¹⁶ evaluated the drying characteristics of concrete in the field and found that even in arid environments, the

internal RH at depths greater than 8 in. (203 mm) was unaffected by ambient conditions due to the low permeability of concrete. Although not measured, the depth to which drying occurs depends on permeability and, therefore, *w/c*. A *w/c* of 0.30 or less would typically result in sufficient desiccation during hydration to reduce the moisture content of the concrete and prevent ASR.¹⁶

Stark¹⁶ and Bérubé et al.⁴ independently determined that an internal RH greater than 80 to 85% (69.8°F [21°C]) was required for ASR to occur for the concrete mixtures, aggregates, and alkali loadings evaluated. Stark¹⁶ determined this value through a combination of lab and field tests. In the lab, mortar bar samples (1 in. [25 mm] square) were subjected to a range of ambient conditions and internal RH assumed equal to ambient RH. In the field, concrete samples were collected at multiple depths within concrete elements, and then stored in hermetically sealed containers at 69.8°F (21°C), followed by measuring the RH above the sample. Bérubé et al.⁴ measured the internal RH for samples stored in the lab by embedding capacitive-type RH probes within concrete cylinders. ASR-related expansion slowed when the internal RH decreased below 80 to 85% (at 69.8°F [21°C]). However, the threshold was shown by Pedneault¹⁹ to depend on the form of siliceous minerals present within the aggregate.

ASR and F/T deterioration in concrete are both dependent on the internal moisture state of concrete. Quantifying the moisture state in concrete as RH has proven a useful index for measuring the efficacy of mitigation. Threshold RH (and VP) values for ASR or F/T deterioration to occur in a concrete specimen can be determined by measuring expansion in concrete at various RH fixing points. These threshold values are applicable to concrete with similar sorption characteristics or when measuring a decrease in RH (or VP) of a concrete structure as compared to a baseline.

Silane sealers

Silanes are low-viscosity penetrating silicon sealers composed of alcohol and alkyl functional groups.²⁰ The hydrophobic and breathable nature of silane sealers makes them promising candidates for treating concrete elements and reducing the internal moisture state. Silanes have been applied to much field concrete as a means of mitigating ASR-related deterioration.^{6,13,14,21-25} The low permeability of concrete may limit the efficacy of silane because drying only occurs in the first 6 to 8 in. (152 to 203 mm) of the exposed surface.¹⁶ Bérubé et al.¹³ and Deschenes et al.¹⁴ found silane reduced ASR- and F/T-related expansion in concrete barriers. Bérubé et al.¹³ measured 0.08% lower expansion in silane-treated barriers as compared to untreated controls. Deschenes et al.¹⁴ measured 0.20% lower expansion in silane-treated barriers that had deteriorated severely due to a combination of ASR and F/T. These results indicate silane treatments slow the progression of combined ASR and F/T deterioration in concrete structures.

Janssen¹¹ also noted that treating F/T-susceptible concrete prisms with silane improved the durability factor (DF) of concrete relative to untreated control specimens. The treatment appeared to slow deterioration of D-cracking-suscep-

tible concrete.¹¹ The average DF increased from 83.7 to 95.3 for water-based silanes, and from 89.6 to 101 for solvent based-silane treatment.¹¹ Bérubé et al.⁴ evaluated silane as a possible means of mitigating combinations of ASR and F/T deterioration in concrete. Silane treatment reduced the moisture state of the concrete (measured as RH) and improved the durability as compared to untreated samples for both non-air-entrained and air-entrained concrete. After 2 years, silane-treated specimens had expanded 0.04%, as compared to 0.18% expansion in the untreated specimens.

Research objectives

Deschenes et al.¹⁴ reported on a field investigation of concrete barriers exhibiting moderate to severe deterioration from a combination of ASR and F/T. The barrier contained the same borderline-reactive aggregate evaluated herein, and the deterioration could not be attributed to ASR alone. Therefore, an investigation to determine the exacerbating effects of F/T on the development of ASR in concrete containing this aggregate was warranted. The fundamental mechanisms of ASR and F/T are well documented and methods for mitigating both are well established. However, understanding the relationships between ASR, F/T, and the moisture state of concrete is important for developing effective mitigation measures for cases of combined deterioration. The objective of this research was thus to better understand the relationship between exposure conditions and combined ASR and F/T deterioration in concrete. More specifically, this work evaluates the effects of storage temperature and ambient RH on the development of ASR in concrete with borderline-reactive and highly reactive aggregates. Additionally, the effects of F/T, moisture state, and silane treatment on the development of ASR were assessed.

RESEARCH SIGNIFICANCE

Understanding the relationship between internal RH, temperature, exposure conditions, and ASR is important in developing durable concrete. This research investigates the threshold RH and VP, at various temperatures, required for ASR deterioration to occur in concretes containing borderline- and highly-reactive aggregates. Specimens containing a borderline-reactive aggregate were also stored in various exposure conditions which accelerate ASR or F/T deterioration. The results indicate concrete with borderline-reactive aggregates can pass required tests for ASR and F/T performance, but deteriorate when exposed to cycles of conditions promoting combinations of ASR and F/T.

EXPERIMENTAL INVESTIGATION

The research was conducted in two phases: the relationship between ambient RH, temperature, and ASR was evaluated first, followed by an investigation of the relationship between ASR, W/D, and F/T.

Relative humidity (RH) and vapor pressure (VP)

Materials—An ASTM C150 Type I/II cement (0.89% Na₂O_{eq}) was used for RH testing. The coarse aggregate was a nonreactive crushed limestone. Two fine aggregates were evaluated: a very-highly-reactive (per ASTM C1778)

Table 1—Materials used for CPT prisms

Material	Highly reactive, lb/yd ³ (kg/m ³)	Borderline-reactive, lb/yd ³ (kg/m ³)	Notes
Cement	708 (420)	708 (420)	0.89% Na ₂ O _{eq}
Coarse aggregate	1782 (1057)	1782 (1057)	Nonreactive limestone
Fine aggregate	1152 (683)	1161 (688)	Reactive aggregate (F.M. = 3.0)
Water	331 (196)	331 (196)	w/c of 0.45
NaOH	3.29 (1.95)	3.29 (1.95)	Na ₂ O _{eq} = 1.25%

Table 2—RH (%) and VP (psi [kPa]) for highly-reactive prisms²⁶⁻²⁸

Salt	NaCl		KCl		KNO ₃		H ₂ O	
	RH	VP, psi (kPa)	RH	VP, psi (kPa)	RH	VP, psi (kPa)	RH	VP, psi (kPa)
Temperature, °F (°C)								
69.8 (21.0)	75.5	0.273 (1.88)	85.8	0.310 (2.14)	93.1	0.336 (2.32)	100	0.363 (2.50)
86.0 (30.0)	75.6	0.467 (3.22)	84.2	0.516 (3.56)	90.6	0.560 (3.86)	100	0.618 (4.26)
104 (40.0)	74.6	0.801 (5.52)	82.4	0.885 (6.10)	88.0	0.944 (6.51)	100	1.07 (7.40)

Table 3—RH (%) and VP (psi [kPa]) for borderline-reactive prisms²⁶⁻²⁸

Salt	NaBr		NaCl		KCl		H ₂ O	
	RH	VP, psi (kPa)	RH	VP, psi (kPa)	RH	VP, psi (kPa)	RH	VP, psi (kPa)
Temperature, °F (°C)								
69.8 (21.0)	58.6	0.212 (1.46)	75.5	0.273 (1.88)	85.8	0.310 (2.14)	100	0.363 (2.50)
86.0 (30.0)	54.6	0.334 (2.33)	75.6	0.467 (3.22)	84.2	0.516 (3.59)	100	0.618 (4.26)
104 (40.0)	49.8	0.535 (3.69)	74.6	0.801 (5.52)	82.4	0.885 (6.10)	100	1.07 (7.40)

siliceous sand with a 1-year concrete prism test (CPT) expansion of 0.550%, and a borderline-reactive (per ASTM C1778) river sand containing chalcedony with a 1-year CPT expansion of 0.040%. The concrete mixtures were designed in accordance with ASTM C1293, and are summarized in Table 1. Sodium hydroxide (NaOH) was added to the concrete mixing water to achieve a total Na₂O_{eq} content of 8.85 lb/yd³ (5.25 kg/m³).

Specimens—Thirty-six concrete prisms were cast for each aggregate tested. The prisms were 3 x 3 x 11.25 in. (75 x 75 x 285 mm), with metal gauge studs embedded at each end for measuring length change. Length change was periodically measured using a length comparator. The highly reactive specimens were monitored for 167 days, and the borderline-reactive specimens for 422 days.

Curing—Three prisms were cast each day, and then cured in the mold for 24 hours at 95% RH (69.8°F [21 °C]). The prisms were then removed from the mold and stored an additional 14 days at 50% RH (69.8°F [21°C]). The specimens were cast over a period of 2 weeks. Therefore, after 14 days of curing, each prism was wrapped in cellophane stored at 32°F (0°C) until all subsequent specimens had cured 14 days.

Exposure conditions—After curing, the prisms were placed in hermetically sealed 6 gal. (23 L) containers with screw-on covers, each capable of holding three prisms. A salt solution was placed in the bottom of each container to control RH within the container. The containers were then stored in a temperature-controlled environment. The containers were periodically moved to an environmental chamber and cooled to 69.8°F (21°C) over a 24-hour period. After cooling, the prisms' length change was measured.

Salt solutions—ACS-grade crystalline salts were used to control RH between 50 and 100%, at temperatures of 69.8,

86, and 104°F (21, 30, and 40°C). The salt solutions, RH, VP, and temperature used for the highly-reactive prisms are summarized in Table 2, and those used for the borderline-reactive prisms are summarized in Table 3. The ambient VP for the storage conditions were calculated using psychrometric equations. The highly reactive aggregate mixture was initially tested with sodium nitrite (NaNO₂) to control RH around 60%. However, the salt was difficult to work with given its toxicity, and results for the prisms are not available. Sodium bromide was used in its place for the borderline-reactive prisms.

The salt solutions were prepared following the recommendations of Wexler and Hasegawa²⁶ and Menzel.¹⁸ Saturated salt solutions were mixed by first boiling 61.0 in.³ (1.0 L) of deionized water, and then mixing crystalline salt into the water until the solution was supersaturated. After the solution cooled to 69.8°F (21°C), additional salt was added to produce a slurry consistency that remained saturated. The solution was then added to each container, and the prisms were suspended above the solution. When the prisms were removed for measurements, additional salt or water was added to the solution to maintain the slurry consistency. The solubility of each salt is dependent on temperature, and additional salt was required for higher temperature storage conditions.

ASR, W/D, and F/T

Materials—An ASTM C150 Type I/II cement (0.96% Na₂O_{eq}) was used for ASR, W/D, and F/T testing, and the total Na₂O_{eq} content was boosted to 8.85 lb/yd³ (5.25 kg/m³). The prisms contained a nonreactive crushed limestone and a borderline-reactive river sand containing chalcedony. To accelerate the development of F/T distress, the concrete was non-air-entrained and contained approximately 2%

entrapped air. The borderline-reactive aggregate used in this study has previously been shown to cause deleterious expansion (0.04%) per ASTM C1293.²⁹ Concrete containing this borderline-reactive sand performs well in the field under normal exposure, but deteriorates when the air content is marginal and exposed to combinations of ASR and F/T.¹⁴ The aggregate was selected to determine if conditions promoting ASR and F/T in the laboratory replicate deterioration observed in the field. The concrete mixture is summarized in Table 4.

Specimens—Fifteen prisms were cast for ASR, W/D, and F/T exposure. The prisms were 3 x 3 x 11.25 in. (75 x 75 x 285 mm), with metal gauge studs embedded at each end for measuring length change. The mass change was also measured to evaluate variations in moisture imparted by the storage conditions. For the ASR, F/T, and F/T + ASR specimens, mass-change was measured after the ASR, F/T, or W cycles, and again after the F/T exposure. For the ASR + F/T + W/D prisms, mass-change was measured after the ASR cycle and again after the drying (D) cycle. Mass and length-change were periodically measured over 300 days.

Curing—The prisms were cured following the same procedure used for RH testing.

Exposure conditions—The storage conditions are summarized in Table 5. The prisms were exposed to 21 cycles intended to accelerate ASR- and/or F/T-related deterioration. Each cycle was 14 days long, including 1 day for measurements. The ASR cycle consisted of 13 days stored at 95% RH and 100°F (38°C) to accelerate ASR, and then 69.8°F (21°C) for 1 day before measurements were taken. The F/T cycle started with 9 days at 95% RH and 69.8°F (21°C) to allow the specimens to absorb moisture but slow ASR. This was followed by measurements, four days of F/T, and additional measurements. Although some ASR likely occurred in the F/T prisms, the rate of reaction is much lower and

F/T deterioration controls. The F/T + ASR cycle started with 9 days at 95% RH 100°F (38°C) to allow the specimens to absorb moisture and accelerate ASR. This was followed by measurements, 4 days of F/T, and additional measurements. The ASR + W/D + F/T cycle started with 7 days stored in containers at 95% RH (100 °F [38 °C]), then 3 days of drying at 50% RH (69.8°F [21°C]), measurements, and finally 3 days of F/T. All the prisms absorbed water while stored at 95% RH, but not directly exposed to liquid water. The prisms were suspended over water in hermetically sealed 6 gal. (23 L) containers with screw-on covers, each holding three prisms.

An F/T chamber was used to rapidly cycle the concrete between 5 and 50°F (−15 and 10°C), at a rate of three cycles per day. The prisms were subjected to F/T cycles at the moisture state produced by the preceding storage at 95% RH. The prisms were not fully saturated during F/T to better represent the deterioration that occurs in concrete in the field. Some drying occurred during F/T, as the prisms were not directly exposed to liquid water.

EXPERIMENTAL RESULTS AND DISCUSSION

Relative humidity (RH) and vapor pressure (VP)

Relative humidity (RH)—The influences of ambient RH, VP, and temperature on the development of ASR were evaluated by storing specimens at combinations of ambient RH and temperature, and periodically measuring strain. An expansion of 0.040% within 1 year for prisms stored at 100% (100°F [38°C]) RH constitutes deleterious expansion per ASTM C1293. Strains exceeding 0.040% may cause cracking for unrestrained concrete. Therefore, a limit of 0.040% strain was selected as the threshold expansion, which constitutes deleterious expansion.

The strain results for prisms containing the highly-reactive aggregate are summarized in Fig. 2. Noting the difference in expansion between Fig. 2(a), 2(b), and 2(c), storage temperature had a greater effect on the development of ASR than ambient RH (or VP). Noting the difference between Fig. 2(a) and 2(c), humidity affects the development of ASR more at higher temperatures than at lower temperatures. The samples stored at 100% RH and 104°F (40°C) (Fig. 2(c)) initially expanded very slowly and then accelerated after 90 days. It is not clear why the expansion was delayed, but may have been due to the process of equilibration. Initially, the degree of saturation was higher due to excess pore water during hydration. As hydration continued and water was adsorbed into hydration products, the moisture state decreased. The moisture state remained low for prisms stored

Table 4—Concrete mixture for prisms subjected to ASR, W/D, and F/T

Material	ASR, W/D, F/T, lb/yd ³ (kg/m ³)	Notes
Cement	708 (420)	0.96% Na ₂ O _{eq}
Coarse aggregate	1800 (1068)	Nonreactive limestone
Fine aggregate	1147 (680)	Borderline-reactive sand
Water	319 (189)	w/c of 0.45
Air	2%	Non-air-entrained
NaOH	2.65 (1.57)	Na ₂ O _{eq} = 1.25%

Table 5—Fourteen-day repeated exposure cycles for ASR, W/D, and F/T

14-day repeated cycles	ASR, days	W, days	LC, days	D, days	F/T, days (cycles)
	100°F (38°C), 95% RH	69.8°F (21°C), 95% RH	69.8°F (21°C)	69.8°F (21°C) 50% RH	−5 to 50°F (−15°C to 10°C)
ASR	13	—	1 (LC, MC)*	—	—
F/T	—	9	1 (LC, MC1)	—	4 (12) (MC2)
F/T + ASR	9	—	1 (LC, MC1)	—	4 (12) (MC2)
ASR + W/D + F/T	7	—	1 (LC, MC1)	3 (MC2)	3 (9)

*Length-change measurement (LC), first mass-change measurement (MC1), second mass-change measurement after drying (MC2).

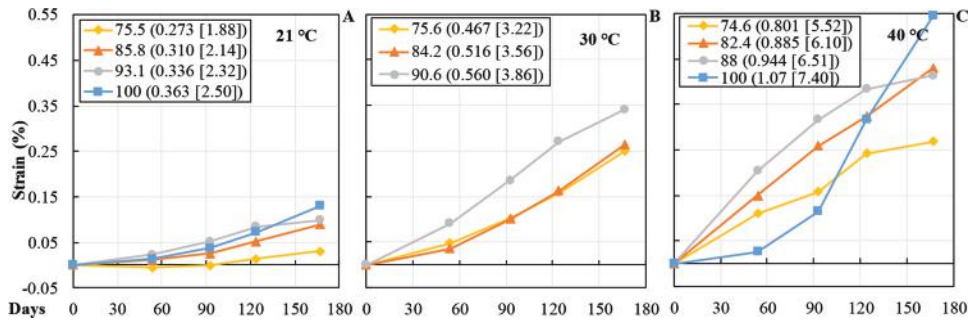


Fig. 2—Strain (%) with respect to time (days), highly reactive fine aggregates. Legend includes RH and VP (psi [kPa]). (Note: °F = 1.8°C + 32.)

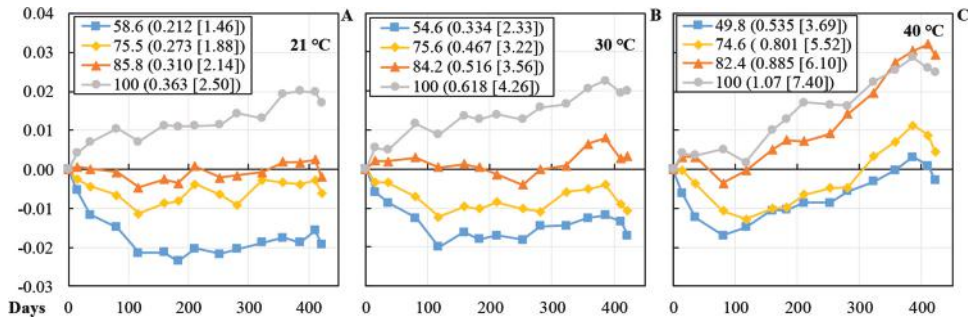


Fig. 3—Strain (%) with respect to time (days), borderline-reactive fine aggregate. Legend includes RH and VP (psi [kPa]). (Note: °F = 1.8°C + 32.)

at low ambient RH. For prisms stored at higher ambient RH, the moisture state increased over time until equilibrium. During this process, gel formation and swelling slowed or ceased during desiccation, but continued when water was transported to the reaction site during equilibration.

Strain results for prisms stored at 69.8°F (21°C) are summarized in Fig. 2(a). The 167-day expansion was 0.030% for prisms stored at 75.5% RH and 0.089% for prisms stored at 85.8% RH. Therefore, a threshold RH may occur between 75.5 and 85.8% for this highly reactive aggregate and alkali loading. This corresponds to a threshold VP between 0.273 and 0.310 psi (1.88 and 2.14 kPa). The samples stored at 75.5% RH contracted slightly over the first 90 days, and then began to expand. This initial contraction was due to drying shrinkage occurring in the concrete. The internal RH of the concrete then reached equilibrium with the ambient RH within 120 days (expansion began).

The results for prisms stored at 86 and 104°F (30 and 40°C) are summarized in Fig. 2(b) and 2(c), respectively. At 167 days, the prisms stored at 86°F (30°C) had expanded between 0.251 and 0.342%, and the prisms stored at 104°F (40°C) had expanded between 0.269 and 0.546%, depending on RH. Noting the expansion for all RH values was greater than 0.040%, it appears a threshold RH does not exist at 86 or 104°F (30 or 40°C) for the range of RH evaluated. As noted in the introduction, the internal RH (and VP) of concrete increases with temperature, and the equilibrium VP within the concrete is higher at 86°F (30°C) than would occur at 69.8°F (21°C). The result is less osmotic pressure required for moisture to be absorbed into the alkali-silica gel product, and greater expansion at the same ambient RH. Another factor that increases the expansion observed

at higher temperatures is the solubility of silica.¹⁹ Noting the difference in expansion between Fig. 2(c) and 2(a), the prisms stored at 100% RH (104°F [40°C]) expanded 0.33% more than those stored at 100% RH (69.8°F [21°C]).

Results for the prisms containing the borderline-reactive aggregate are summarized in Fig. 3(a), 3(b), and 3(c). The prisms evaluated herein appear to reach equilibrium with the ambient storage conditions within 120 days (when expansion or contraction becomes stable).

The strain results for prisms stored at 69.8°F (21°C) are summarized in Fig. 3(a). The prisms stored at 85.8% RH (0.310 psi [2.14 kPa]) show no dilation or contraction, indicating the prisms had an initial internal RH close to this value. The prisms stored at 100% RH (0.363 psi [2.50 kPa]) expanded 0.011% within 80 days and then remained stable until 323 days, followed by expansion to 0.020% over the remaining 100 days. The prisms stored at 58.6 and 75.5% RH (0.212 and 0.273 psi [1.46 and 1.88 kPa]) contracted and became stable once equilibrium occurred between internal and ambient RH.

The strain data for prisms stored at 86°F (30°C) are summarized in Fig. 3(b). The prisms also reached equilibrium within 120 days and then remained stable until 323 days. The prisms stored at 84.2% RH (0.516 psi [3.56 kPa]) expanded 0.008%, and those stored at 100% RH (0.618 psi [4.26 kPa]) expanded 0.023%. The prisms stored at 54.6% RH (0.334 psi [2.33 kPa]) and 75.6% RH (0.467 psi [3.22 kPa]) contracted for 120 days and then became stable. This indicates that desiccation and drying shrinkage occurred for prisms stored at 75.6% RH and lower, while absorption and expansion occurred at 84.2% and higher.

The results for prisms stored at 104°F (40°C) are summarized in Fig. 3(c). The prisms stored at 49.8% RH (0.535 psi [3.69 kPa]) initially contracted and then expanded to 0.003%. Similarly, the prisms stored at 74.6% RH (0.801 psi [5.52 kPa]) contracted and then expanded to 0.011%. The prisms stored at 82.4% RH (0.885 psi [6.10 kPa]) reached a maximum expansion of 0.032%, and those stored at 100% RH (1.07 psi [7.40 kPa]) expanded 0.029%. Expansion occurred for all the prisms, indicating absorption and ASR formation occurred when RH was greater than 49.8%. The results generally indicate that expansion increases with RH and VP. However, this trend was broken by the prisms stored at higher temperature and lower RH. The prisms may have lost internal moisture more rapidly from desiccation, resulting in lower overall expansion despite higher internal VP.

The ambient RH required to cause deleterious expansion (that is, >0.04%), for the borderline aggregate and alkali loading, appears to be greater than 100% RH (104°F [40°C]), corresponding to a VP greater than 1.07 psi [7.40 kPa]. The 1-year CPT expansion for the borderline-reactive aggregate samples stored was previously measured at 100% RH (100°F [38°C]) and ranged from 0.025 to 0.040%, depending on the inert coarse aggregate used in combination with the reactive sand.²⁹ This aggregate has caused ASR and deleterious expansion in the field and in laboratory concretes, confirmed through petrographic examination.^{25,29} The lower expansion measured herein may be due to alkali-leaching from the prisms stored at 86 and 104°F (30 and 40°C). Minor temperature fluctuations cause condensation of moisture on the concrete prisms, which can lead to alkali leaching, and reduced overall expansion.³⁰ This potentially explains why expansion slows and then stops after 380 days for prisms stored at 100% RH and 82.4% (104°F [40 °C]) (Fig. 3(c)).

Vapor pressure (VP)—The data were also plotted as strain with respect to VP, as summarized in Fig. 4. The data were plotted for several measurement days over the monitoring period to highlight the change in coefficient of determination (R^2) over time. The data for the prisms containing highly reactive sand are summarized in Fig. 4(a). The results indicate R^2 increases with time, along with the slope. As observed from Fig. 2(c), the rate of strain slows after 124 days and the slope of the strain with respect to VP increases less between 124 and 167 days. The best correlation for the highly reactive prisms occurred at 167 days, with an R^2 of 0.876. The equation of the trendline was determined and used to calculate the point where the line intercepts a strain of 0.04%. This occurred at a VP of 0.180 psi (1.24 kPa), which corresponds to a RH of 50.0% (69.8°F [21°C]). Given the high reactivity of this concrete mixture, such a threshold seems reasonable.

VP results for prisms containing the borderline-reactive sand are summarized in Fig. 4(b). Comparing the rates of expansion (slope) between Fig. 4(a) and 4(b), the reactivity of the mixture has a greater effect on strain than the storage conditions. The coefficient of determination increases with time until 386 days, after which it begins to decrease. Noting the strain with respect to time for this aggregate shown in Fig. 3(a) to 3(c), the prisms begin to contract after 386 days. This was attributed to the slowing rate of reaction after 380 days. The equation relating 386-day strain to VP had an R^2

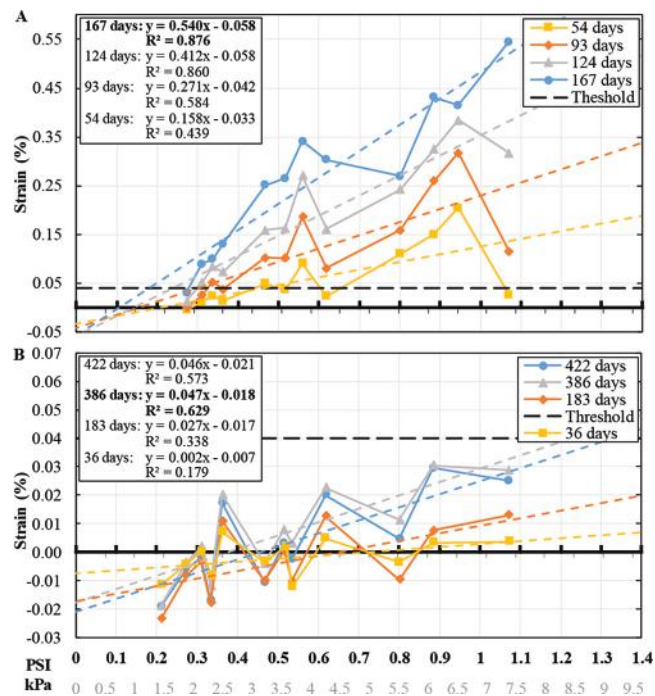


Fig. 4—Strain (%) with respect to VP (psi, bold axis [kPa, secondary axis]): (a) highly reactive fine aggregate; and (b) borderline-reactive fine aggregate.

of 0.629, and was used to calculate a threshold VP. Based on the 386-day results, this concrete would require a VP of 1.22 (8.47 kPa) to achieve an expansion of 0.04%. This VP corresponds to a RH of 100% (108.7°F [42.6°C]). A lower threshold may be expected for a concrete containing the same aggregate at a higher alkali loading or different coarse aggregates. Prisms containing the same fine aggregate and alkali loading were tested in combination with a granite coarse aggregate and developed deleterious expansion at a VP of 0.962 psi (6.63 kPa) corresponding to 100% RH at 100°F (38°C). The development of ASR and expansion at low ambient RH and temperature may be explained by loss of moisture and increased pore solution alkalinity. This hypothesis is based on the nature of cement paste and the physics of water in colloidal gels (C-S-H). However, validation requires additional testing over a broader range of fixed internal VPs. As the rate of hydration slows and the cement pores are no longer saturated, the concentration of alkalis remaining in solution increases when water evaporates out of the pore solution, leaving cations behind. The siliceous minerals become soluble in the presence of a higher concentration of hydroxyl ions, resulting in the development of alkali-silica gel and transport of pore solution into the alkali-silica gel. As a result, alkali-silica gel develops in the presence of the concentrated solution, and water is absorbed into the alkali-silica gel. The concentration of alkalis eventually decreases due to alkali-leaching, until the development of alkali-silica gel ceases. The curvature of the menisci within the pores of the cement paste increases (and VP decreases) as water is absorbed into alkali-silica gel and evaporates due to drying. Due to the lower VP, water is transported from the capillary spaces into the pores of the paste. This continues until the RH (and VP) within the pores of the paste is in equi-

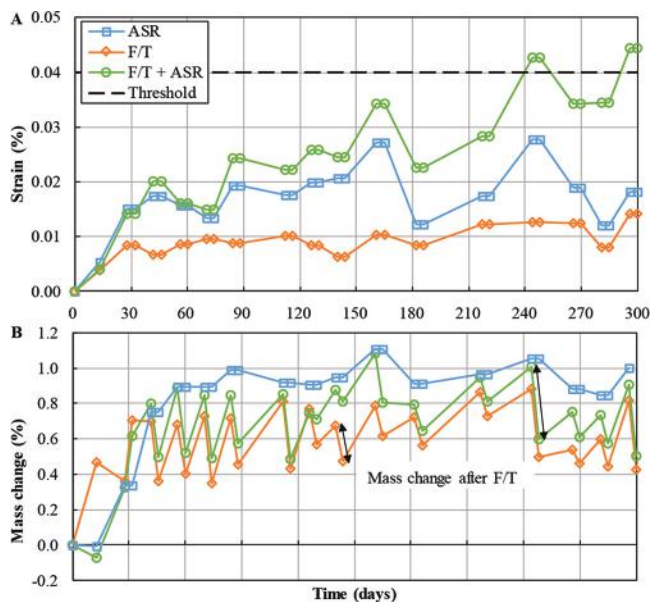


Fig. 5—(a) Strain (%); and (b) mass change with respect to time (days), concrete prisms exposed to conditions that accelerate ASR, F/T, or ASR and F/T.

librium with the ambient conditions. If the equilibrium RH is sufficiently low, the osmotic pressure required for water to be absorbed from the pore solution into the alkali-silica gel is greater than the VP in the pores of the paste, and expansion cannot be sustained. This threshold pressure depends on the osmotic pressure exerted by the alkali-silica gel, which varies with the solubility of silica and the gradient between the concentration of ions in solution and those in the alkali-silica gel.¹⁹

ASR, W/D, F/T

The results of strain and mass change measurements for ASR, W/D, and F/T testing are summarized in Fig. 5 and 6. From Fig. 5(a), the prisms stored at 95% RH (100°F [38°C]) expanded 0.027% within 165 days, and then contracted to 0.012%. This was followed by expansion to 0.028%, contraction to 0.012%, and finally expansion to 0.18%. There was no clear reason for this cyclic trend in stain. The prisms were stored at a constant temperature and RH throughout the monitoring period, except for 24 hours of cooling before measuring strain. The mass-change results (Fig. 5(b)) reveal a minor decrease (0.2%) in mass during these periods of contraction, which may have contributed to the contraction measured in the samples.

The prisms exposed to 160 F/T cycles expanded to 0.009% within 30 days and then slowly expanded to a final expansion of 0.014%, fluctuating due to cyclic exposure conditions. The initial expansion is partly due to moisture gain caused by the 0.47% increase in mass within the first 30 days (Fig. 5(b)). The remaining expansion is due to F/T deterioration. In comparison, the prisms exposed to F/T + ASR were subjected to 175 days at 95% RH (100°F [38°C]) and 160 F/T cycles, with a final expansion of 0.045%. Despite being exposed to 125 less days of conditions that accelerate ASR, the F/T + ASR prisms exhibited 0.026% greater expansion than the ASR prisms and 0.031% greater expansion than the

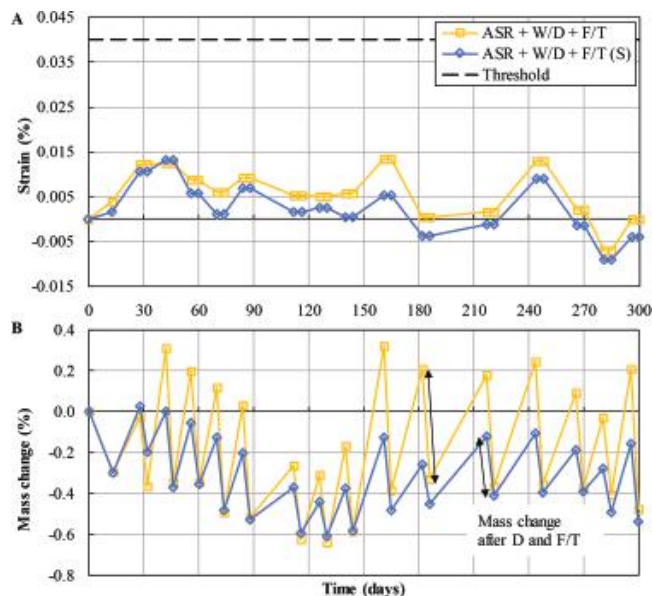


Fig. 6—(a) Strain (%); and (b) mass change with respect to time (days), concrete prisms exposed to conditions that accelerate combination of ASR and F/T.

F/T prisms. This indicates that cycles of conditions accelerating ASR and F/T exacerbated deterioration relative to ASR or F/T alone. The F/T + ASR prisms also contracted after 165 days, followed by expansion and another cycle of contraction after 248 days. The final strain after 300 days of monitoring was 0.045%. The cycles in expansion and contraction align with those measured in the ASR prisms and correspond to a decrease in mass. The only likely reasoning for this decrease in mass is drying. Despite the cycles of expansion and contraction, the F/T, ASR, and F/T + ASR prisms had a trend of increasing expansion over the monitoring period.

Mass change was measured before and after drying, and the results are summarized in Fig. 5(b). The prisms exposed to ASR, F/T, and F/T + ASR absorbed ~0.6% moisture by mass within the first 45 days and then varied with cycles throughout the test duration. Some drying occurred during F/T due to the lower humidity within the F/T chamber. The average mass change was -0.23% during F/T followed by and increase back to 0.75% after storage at 95% RH.

The F/T prisms were exposed to 9 days at 95% RH (69.5°F [21°C]) and absorbed slightly less (~0.1%) water than the F/T + ASR prisms exposed to 9 days at 95% RH (100°F [38°C]). This difference may be attributed to additional moisture absorbed by the concrete stored at higher temperatures. However, the mass change of the ASR prisms did not increase appreciably compared to those exposed to F/T + ASR, and the difference in expansion measured for the ASR + F/T samples is likely due to the formation of microcracks and deterioration rather than absorption of water.

The samples exposed to conditions accelerating either ASR or F/T did not develop deleterious expansion over the monitoring period. However, samples exposed to a combination of F/T + ASR developed deleterious expansion (>0.04%) and exhibited an expansive trend within the same period. No available standardized laboratory test method would deem this concrete unfit for use in the field. Field

performance records indicate that concrete containing this borderline-reactive aggregate deteriorated when exposed to conditions promoting ASR in the summer and F/T in the winter.¹⁴ Bérubé et al.⁴ also observed that combinations of ASR and F/T exacerbate deterioration as compared to ASR or F/T alone. Bérubé et al.⁴ included specimens with air entrainment exposed to similar cycles of ASR and F/T and found deterioration to increase as compared to cylinders exposed to ASR or F/T alone. However, the highly reactive coarse aggregate used in Bérubé et al.⁴ rapidly developed deleterious ASR expansion, which makes the deterioration contribution of F/T less apparent.

The prisms exposed to ASR + W/D + F/T (Fig. 6(a)) exhibited less than 0.013% expansion after 300 days of monitoring as compared to 0.045% for prisms exposed to ASR + F/T (Fig. 5(a)). Based on the mass-change results, it appears drying (Fig. 6(b)) prevented both ASR and F/T deterioration. The prisms treated with silane [ASR + W/D + F/T (S)] exhibited similar behavior on drying (Fig. 6(a)). On rewetting, the untreated prisms absorbed an average 0.28% (by mass) more water than silane-treated prisms. The cyclic expansion and contraction measured in the prisms was likely due to moisture gain and loss, rather than gel or crack formation. Interestingly, the only difference between the ASR + W/D + F/T (Fig. 5) and the F/T + ASR samples (Fig. 6) was the additional drying time. The additional period of drying reduced the moisture state of the concrete and prevented ASR and F/T deterioration.

CONCLUSIONS AND RECOMMENDATIONS

Relative humidity (RH) and vapor pressure (VP)

- The threshold RH required for deleterious ASR to occur in concrete, at a given alkali loading, depends on temperature and the reactive form of silica present within the aggregate. The prisms containing a highly reactive sand in this study exhibited a threshold RH less than 80% (69.8°F [21°C]). The prisms stored at combinations of RH and temperature above this value showed deleterious expansion within 167 days.
- Comparing VP may be more intuitive for developing threshold values for ASR. VP is a function of RH and temperature, and can be directly measured using commercial RH probes. Alternatively, it can be calculated from RH and temperature measurements. Determining threshold VP may be useful for evaluating mitigation measures in the field, where controlling the internal moisture state of concrete is necessary for slowing ASR- and/or F/T-related deterioration. VP can be compared at a range of ambient temperatures, rather than specific temperatures such as 69.8°F (21°C).

ASR, W/D, F/T

- The test conditions used in this study appear to better replicate the combined ASR and F/T deterioration observed in the field. The borderline-reactive aggregate used in this study often passes ASTM C1293. The aggregate has been associated with ASR- and F/T-related expansion in a concrete barrier wall.^{14,29} Prisms

containing the borderline-reactive aggregate were exposed to conditions accelerating ASR and F/T, and expanded more than prisms exposed to conditions accelerating ASR or F/T alone.

- Prisms exposed to cycles of W/D (Fig. 5) expanded less than 0.013% as compared to expansions ranging from 0.014 to 0.045% for prisms subjected to ASR and/or F/T (Fig. 6). Drying reduced the moisture state of the concrete, protecting the concrete from expansive deterioration during conditions that accelerate ASR or F/T. In addition, prisms treated with silane and exposed to cycles of ASR + W/D + F/T expanded less and absorbed significantly less water than untreated prisms.
- Concrete containing the borderline-reactive aggregates and exposed to seasons of warm, humid conditions, which accelerate ASR, followed by seasons of daily F/T cycles, may deteriorate faster than concrete exposed to conditions promoting ASR or F/T alone. Air entrainment alone cannot prevent deterioration in concrete containing a combination of reactive and D-cracking-susceptible aggregates. Additional preventative measures may be required to limit the development of alkali-silica gel, and to reduce the moisture state of concrete during F/T.

AUTHOR BIOS

ACI member Richard A. Deschenes Jr. is an Assistant Professor at Youngstown State University, Youngstown, OH. He received his PhD in civil engineering from the University of Arkansas, Fayetteville, AR, in 2017. He also received the 2013 ACI Schwing American Scholarship and the 2015 ACI BASF Construction Chemicals Fellowship. His research interests include concrete materials and durability of concrete.

ACI member Eric R. Giannini is a Principal Investigator with RJ Lee Group, Inc., Monroeville, PA. He received his PhD in civil engineering from The University of Texas at Austin, Austin, TX, in 2012. He is a member of ACI Committees 123, Research and Current Developments; 201, Durability of Concrete; 228, Nondestructive Testing of Concrete; and S802, Teaching Methods and Educational Materials. His research interests include alkali-silica reaction and nondestructive testing.

ACI member Thanos Drimalas is a Research Associate in the Department of Civil, Architectural, and Environmental Engineering at the University of Texas at Austin, where he received his PhD in civil and environmental engineering in 2007. He is a member of ACI Committees 201, Durability of Concrete; and 350, Environmental Engineering Concrete Structures. His research interests include durability of concrete materials and alkali-aggregate reaction.

Benoit Fournier is a Professor in the Department of Geology and Geological Engineering at Université Laval, Quebec, QC, Canada. He is a member of ACI Committee 201, Durability of Concrete. His research interests include aggregate technology, durability of concrete, alkali-aggregate reactions, and incorporating SCMs.

W. Micah Hale, FACI, is Professor and Head of the Department of Civil Engineering at the University of Arkansas. He received his BS, MS, and PhD in civil engineering from the University of Oklahoma, Norman, OK. He is Chair of ACI Committee 363, High-Strength Concrete, and is a member of ACI Committees 233, Ground Slag in Concrete; 239, Ultra-High-Performance Concrete; and Joint ACI-ASCE Committee 423, Prestressed Concrete. His research interests include concrete materials, mixture proportioning, and prestressed concrete.

REFERENCES

1. Powers, T. C., and Steinour, H. H., "An Interpretation of Some Published Researches on the Alkali-Aggregate Reaction, Part 1—The Chemical Reactions and Mechanism of Expansion," *ACI Journal Proceedings*, V. 52, No. 6, June, 1955, pp. 497-516.

2. Chatterji, S., "Mechanisms of Alkali-Silica Reaction and Expansion," *Proceedings of the 8th International Conference on Alkali-Aggregate Reaction (ICAAAR)*, Kyoto, Japan, 1989, pp. 101-105.
3. Diamond, S., "ASR—Another Look at Mechanisms," *Proceedings of the 8th International Conference on Alkali-Aggregate Reaction (ICAAAR)*, Kyoto, Japan, 1989, pp. 83-94.
4. Bérubé, M.-A.; Chouinard, D.; Pigeon, M.; Frenette, J.; Boisvert, L.; and Rivest, M., "Effectiveness of Sealers in Counteracting Alkali-Silica Reaction in Plain and Air-Entrained Laboratory Concretes Exposed to Wetting and Drying, Freezing and Thawing, and Salt Water," *Canadian Journal of Civil Engineering*, V. 29, No. 2, 2002, pp. 289-300. doi: 10.1139/102-011
5. Nishibayashi, S.; Yamura, K.; and Sakata, K., "Evaluation of Cracking of Concrete due to Alkali-Aggregate Reaction," *Proceedings of the 8th International Conference on Alkali-Aggregate Reaction (ICAAAR)*, Kyoto, Japan, 1989, pp. 759-764.
6. Fournier, B.; Bérubé, M.-A.; Folliard, K. J.; and Thomas, M. D. A., "Report on the Diagnosis, Prognosis, and Mitigation of Alkali-Silica Reaction (ASR) in Transportation Structures," *Report No. FHWA-HIF-09-004*, Federal Highway Administration, U.S. Department of Transportation, Washington, DC, 2010, 154 pp.
7. Courtier, R. H., "The Assessment of ASR-Affected Structures," *Cement and Concrete Composites*, V. 12, No. 3, 1990, pp. 191-201. doi: 10.1016/0958-9465(90)90020-X
8. Powers, T. C., "A Working Hypothesis for Further Studies of Frost Resistance of Concrete," *ACI Journal Proceedings*, V. 42, No. 4, Apr. 1945, pp. 245-272.
9. Powers, T. C., and Helmuth, R. A., "Theory of Volume Changes in Hardened Portland-Cement Paste during Freezing," *Proceedings of the Annual Meeting—Highway Research Board*, V. 32, 1953, pp. 285-297.
10. Powers, T. C., "Freezing Effects in Concrete," *Durability of Concrete*, SP-47, C. F. Scholer and E. Farkas, eds., American Concrete Institute, Farmington Hills, MI, 1975, pp. 1-11.
11. Janssen, D. J., and Snyder, M. B., "Resistance of Concrete to Freezing and Thawing," No. SHRP-C-391, National Research Council, Washington, DC, 1994, 217 pp.
12. Litvan, G. G., "Phase Transitions of Adsorbates, IV, Mechanism of Frost Action in Hardened Cement Paste," *American Ceramic Society Journal*, V. 55, No. 1, 1972, pp. 38-42. doi: 10.1111/j.1151-2916.1972.tb13393.x
13. Bérubé, M.-A.; Chouinard, D.; Pigeon, M.; Frenette, J.; Rivest, M.; and Vezina, D., "Effectiveness of Sealers in Counteracting Alkali-Silica Reaction in Highway Median Barriers Exposed to Wetting and Drying, Freezing and Thawing, and Deicing Salt," *Canadian Journal of Civil Engineering*, V. 29, No. 2, 2002, pp. 329-337. doi: 10.1139/102-010
14. Deschenes, R. Jr.; Murray, C. D.; and Hale, W. M., "Mitigation of Alkali-Silica Reaction and Freezing and Thawing through Surface Treatment," *ACI Materials Journal*, V. 114, No. 2, Mar.-Apr. 2017, pp. 307-314. doi: 10.14359/51689493
15. Rust, C., "Role of Relative Humidity in Concrete Expansion due to Alkali-Silica Reaction and Delayed Ettringite Formation: Relative Humidity Thresholds, Measurement Methods, and Coatings to Mitigate Expansion," MS thesis, The University of Texas at Austin, Austin, TX, 2009, 120 pp.
16. Stark, D., "The Moisture Condition of Field Concrete Exhibiting Alkali-Silica Reactivity," *CANMET/ACI International Workshop on Alkali-Aggregate Reaction in Concrete*, Halifax, NS, Canada, 1990, 19 pp.
17. Gause, R. G., and Tucker Jr., J., "Method for Determining the Moisture Condition in Hardened Concrete," *Journal of Research of the National Bureau of Standards*, V. 25, Oct. 1940, 14 pp.
18. Menzel, C. A., "A Method for Determining the Moisture Condition of Hardened Concrete in Terms of Relative Humidity," *ASTM Proceedings*, V. 55, 1955, pp. 1-26.
19. Pedneault, A., "Development of Testing and Analytical Procedures for the Evaluation of the Residual Potential of Reaction, Expansion, and Deterioration of Concrete Affected by ASR," MSc memoir, Laval University, Québec City, QC, Canada, 1996, 133 pp.
20. Mayer, H., "The Chemistry and Properties of Silicone Resins: Network Formers (in Paints and Renders)," *Pigment & Resin Technology*, V. 27, No. 6, 1998, pp. 364-373. doi: 10.1108/03699429810246953
21. Kobayashi, A.; Kirimura, K.; Kuboyama, K.; and Kojima, T., "Evaluation of Surface Treatment Effect for Preventing Excessive Expansion due to Alkali-Silica Reaction," *Proceedings of the 8th International Conference on Alkali-Aggregate Reaction (ICAAAR)*, Kyoto, Japan, 1989, pp. 821-826.
22. Bérubé, M. A.; Chouinard, D.; Boisvert, L.; Frenette, J.; and Pigeon, M., "Influence of Wetting-Drying and Freezing-Thawing Cycles, and Effectiveness of Sealers on ASR," *Proceedings of the 10th International Conference on Alkali-Aggregate Reaction (ICAAAR)*, Melbourne, Australia, 1996, pp. 1056-1063.
23. Folliard, K. J.; Thomas, M. D. A.; Fournier, B.; Resendez, Y.; Drimalas, T.; and Bentivegna, A., "Evaluation of Mitigation Measures Applied to ASR-Affected Concrete Elements: Preliminary Findings from Austin, TX Exposure Site," *Proceedings of the 14th International Conference on Alkali Aggregate Reaction (ICAAAR)*, Austin, TX, 2012, 10 pp.
24. Thomas, M. D. A.; Folliard, K. J.; Fournier, B.; Drimalas, T.; and Rivard, P., "Study of Remedial Actions on Highway Structures Affected by ASR," *Proceedings of the 14th International Conference on Alkali-Aggregate Reaction (ICAAAR)*, Austin, TX, 2012, 10 pp.
25. Thomas, M. D. A.; Folliard, K. J.; Fournier, B.; Rivard, P.; and Drimalas, T., "Methods for Evaluating and Treating ASR-Affected Structures: Results of Field Application and Demonstration Projects," *Report No. FHWA-HIF-14-0002*, Federal Highway Administration, U.S. Department of Transportation, Washington, DC, 2013, 80 pp.
26. Wexler, A., and Hasegawa, S., "Relative Humidity-Temperature Relationships of Some Saturated Salt Solutions in the Temperature Range 0 Degree to 50 Degrees C," *Journal of Research of the National Bureau of Standards*, V. 53, No. 1, 1954, pp. 19-26. doi: 10.6028/jres.053.003
27. Rockland, L. B., "Saturated Salt Solutions for Static Control of Relative Humidity between 5° and 40°C," *Analytical Chemistry*, V. 32, No. 10, 1960, pp. 1375-1376. doi: 10.1021/ac60166a055
28. Greenspan, L., "Humidity Fixed Points of Binary Saturated Aqueous Solutions," *Journal of Research of the National Bureau of Standards. Section A. Physics and Chemistry*, V. 81A, No. 1, 1977, pp. 89-96. doi: 10.6028/jres.081A.011
29. Deschenes, R. Jr., and Hale, W. M., "Alkali-Silica Reaction in Concrete with Previously Inert Aggregates," *Journal of Performance of Constructed Facilities*, V. 21, No. 2, Apr. 2017, pp. 1-10.
30. Rogers, C. A., and Hooton, R. D., "Reduction in Mortar and Concrete Expansion with Reactive Aggregates Due to Alkali Leaching," *Cement, Concrete and Aggregates*, V. 13, No. 1, 1991, pp. 42-49. doi: 10.1520/CCA10548J